

Fig. S1. Frequency spectra of angular changes in head direction of the study animals during 13 target approach sequences. Strong head turns (>5 deg) do not occur at rates higher than approximately 1.5 Hz, making them detectable when sampling at 5 Hz (i.e. with a Nyquist frequency of 2.5 Hz, indicated by the vertical dashed line).

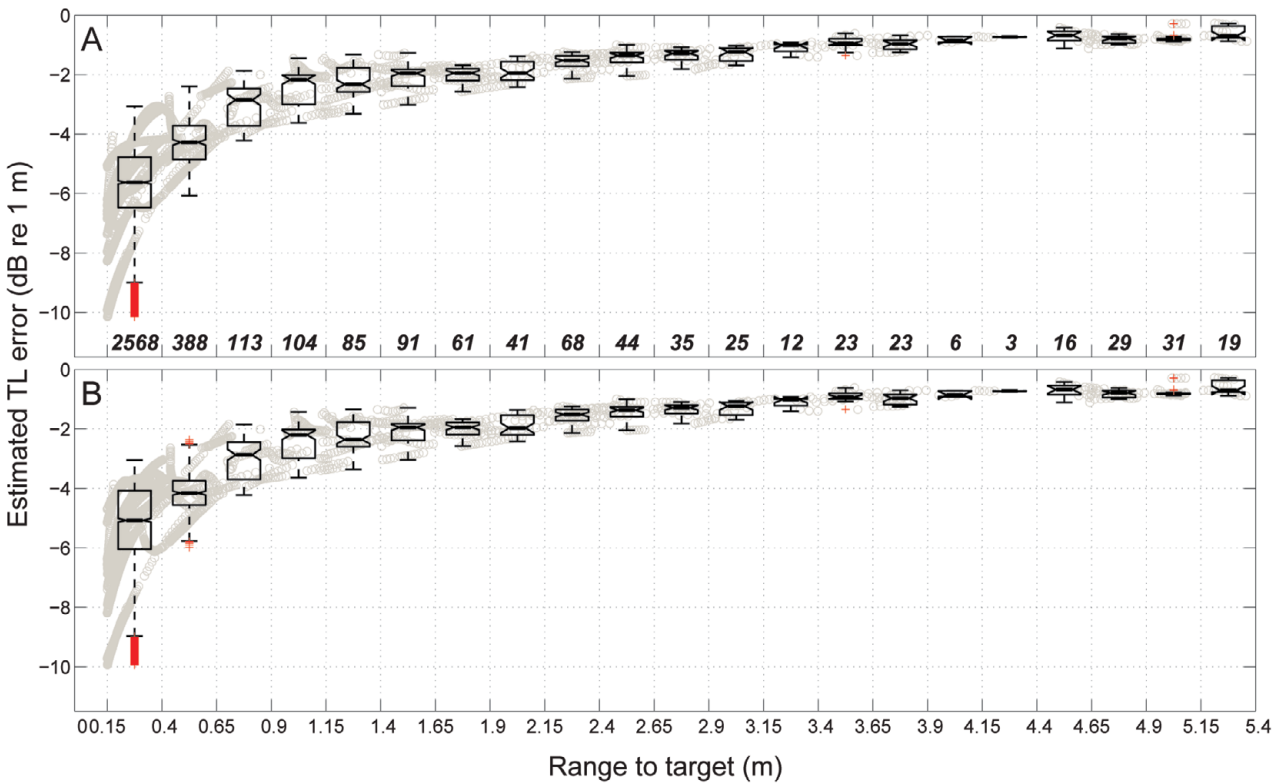


Fig. S2. Transmission loss (TL) error for the video-based range estimates computed at (A) 25 and (B) 5 frames s^{-1} . The animals' positions were obtained by combining the overhead and underwater (sampled always at 25 frames s^{-1}) video tracks. Estimates from video-based tracking were compared with the ranges obtained from the time of arrival differences between the outgoing clicks and the returning echoes recorded on the tag. Pooled data points from 13 trials were grouped into 25-cm-wide range bins to produce notched box plots representing the 25th, 50th (median) and 75th percentile of relative errors within each range bin. Whiskers extend to the extreme values within 1.5 interquartile ranges and outliers are plotted individually in red. Numbers in the lower part of A give the sample size per range bin. Because the TL error depends on the distance to the target, at short ranges errors on the order of a few centimeters make a relatively large contribution. Therefore, the last 15 cm of data (corresponding roughly to the length of a porpoise rostrum) have been excluded both here and in the analysis of apparent source level and inter-click interval adjustments. As tracks generated at 5 frames s^{-1} gave rise to a smaller error, for the remaining data we only estimated the animals' positions for every fifth frame of the overhead video and combined it with every single frame of the underwater camera recordings.

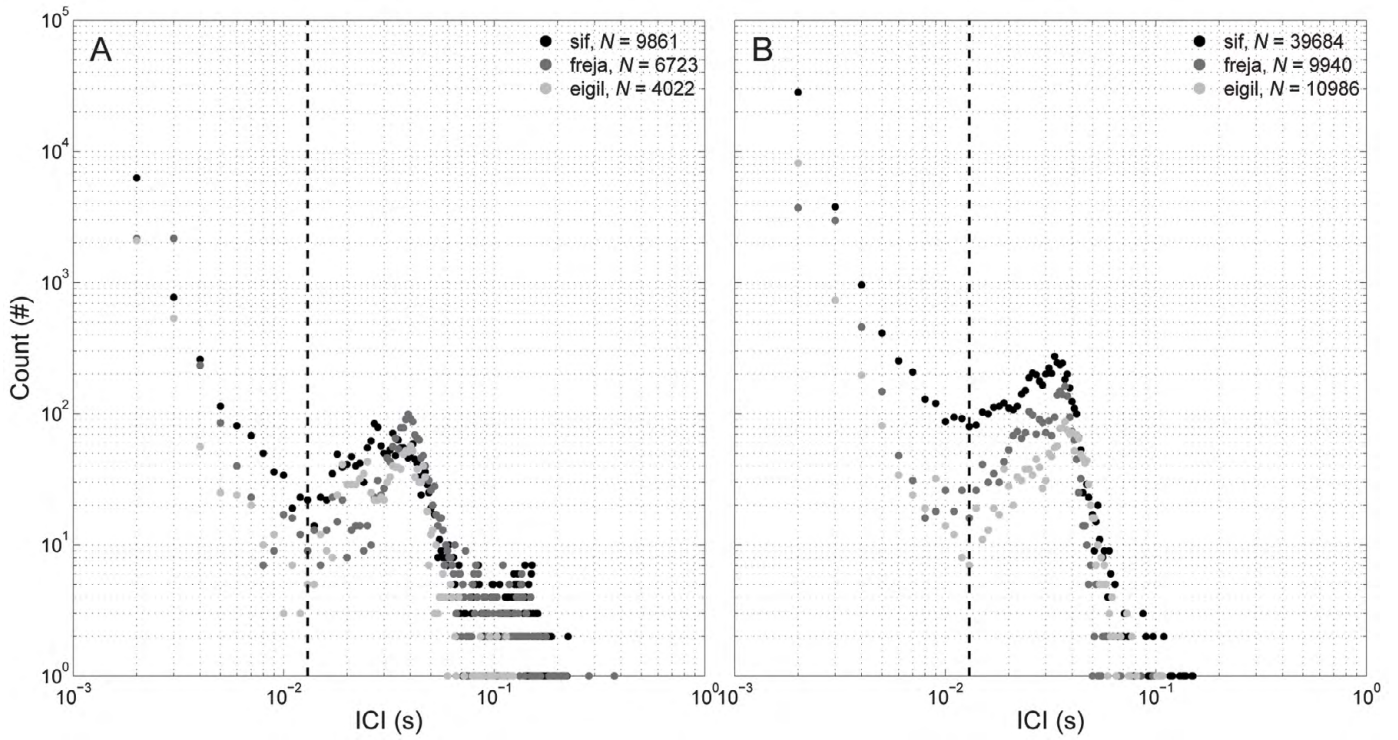


Fig. S3. Distribution of inter-click intervals (ICIs) detected (A) on the tag and (B) on the target hydrophones for the three porpoises. Bin width is 1 ms. Only on-target clicks, i.e. clicks with received levels within 6 dB of the peak levels in scans, have been included in B. The peaks centered on around 2 ms correspond with the dominant ICIs for buzz clicks. The peaks between 25 and 45 ms mark the dominant ICI range for regular clicks adjusted to the relatively short range targets. The third group of peaks centered above 100 ms explicit on the tag, but absent from the target hydrophone, data corresponds to off-target clicks, that either are directed and adjusted to long-range targets, or signify gaze opening. The vertical dashed line at 13 ms denotes the upper limit of ICI used to define buzz clicks.

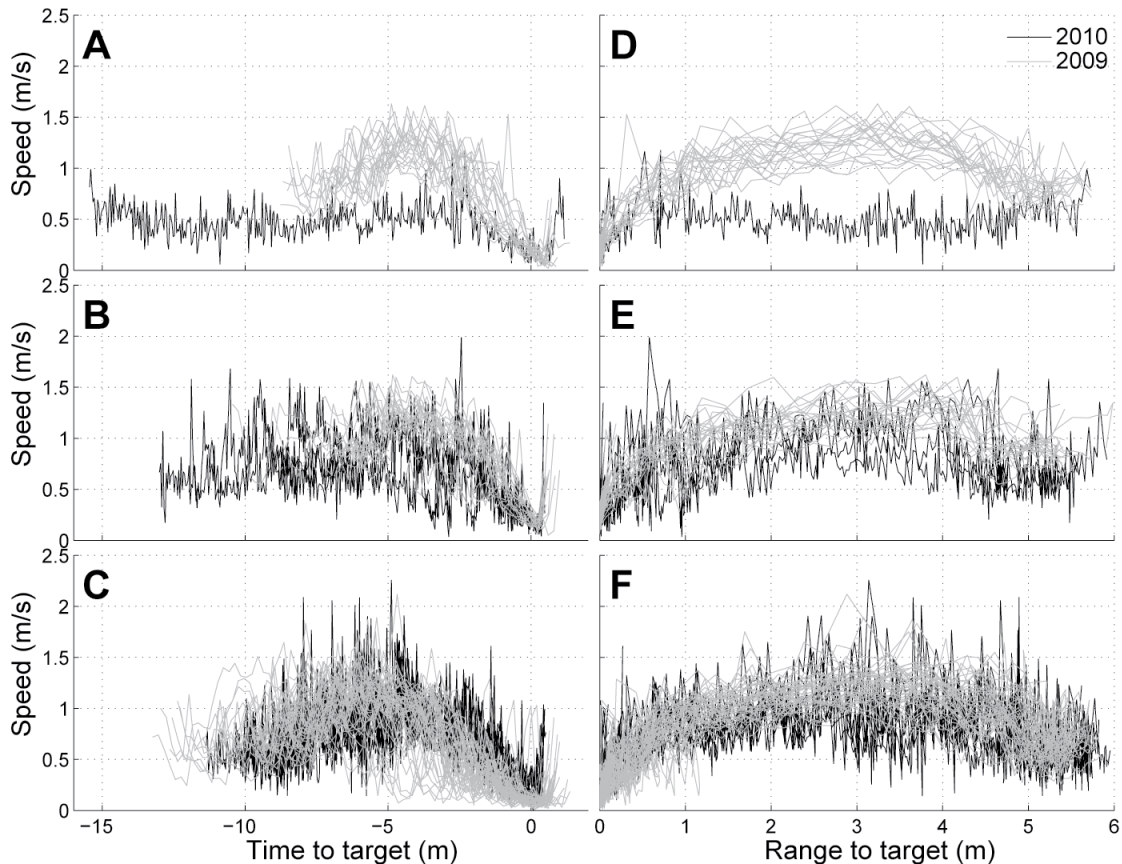


Fig. S4. Speed of the three animals computed by differentiating the range between each point in a track (see Fig. 2 for track examples). (A,D) Eigil, (B,E) Freja and (C,F) Sif. Data from the first set of recordings in 2009 are presented in grey, and data collected in 2010 are shown in black.

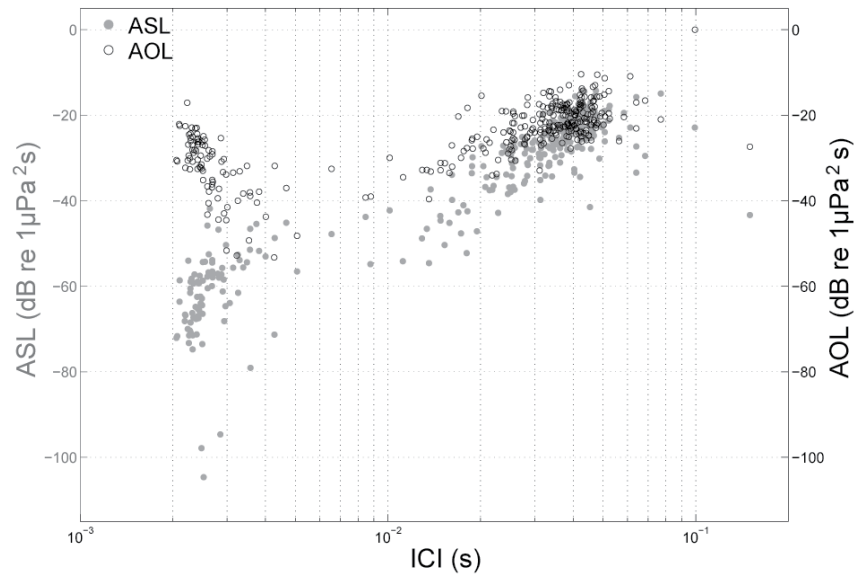


Fig. S5. Bi-modal distribution of the range-dependent parameters of the target-directed echolocation clicks. Normalized apparent source levels (ASLs) of the on-axis clicks back-calculated from the received levels at the target hydrophones are plotted against the delay since last click (ICI) for 236 regular and 94 buzz clicks from 13 trials with tagged animals. Also shown are the apparent output levels (AOLs) of the same clicks recorded on the tag and plotted against the ICI. The signals were classified as buzz or regular according to the criterion illustrated in supplementary material Fig. S3. Only clicks produced at ranges greater than 15 cm are presented here.

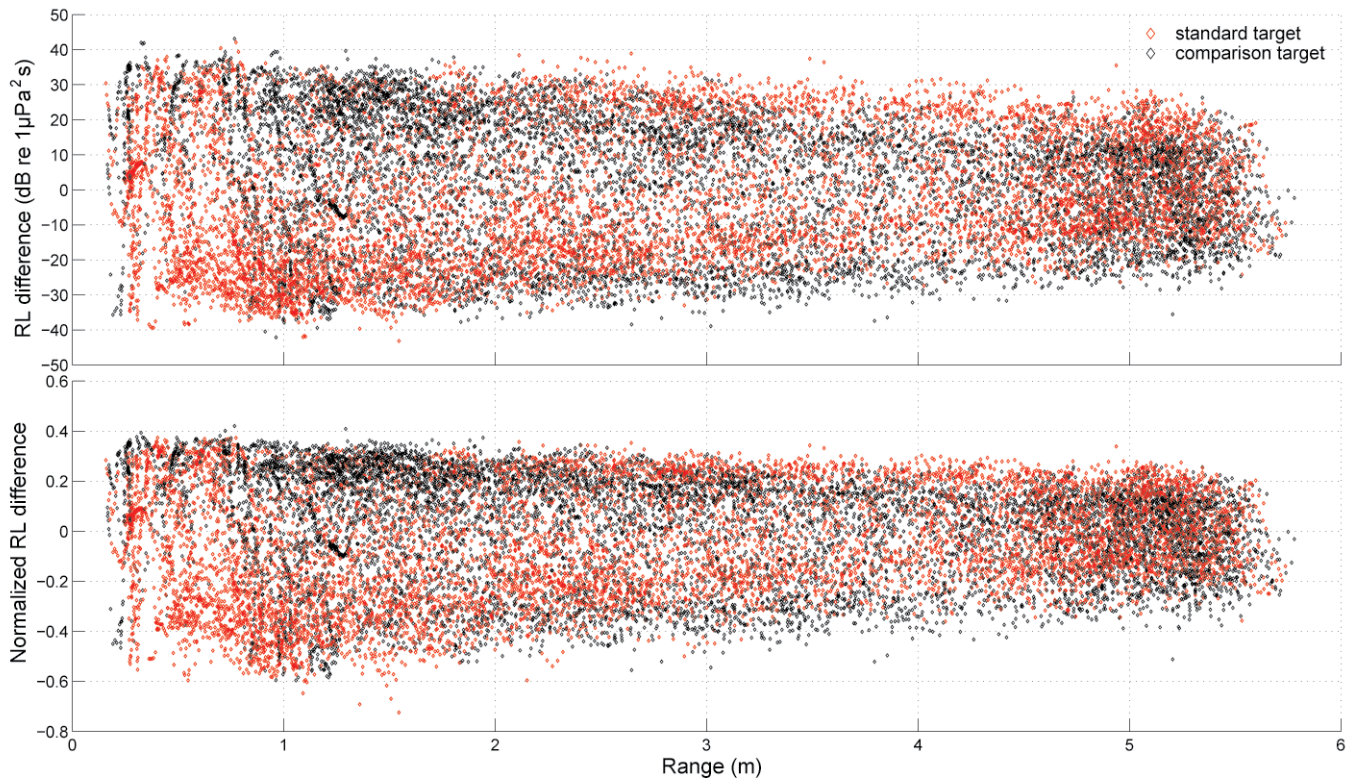
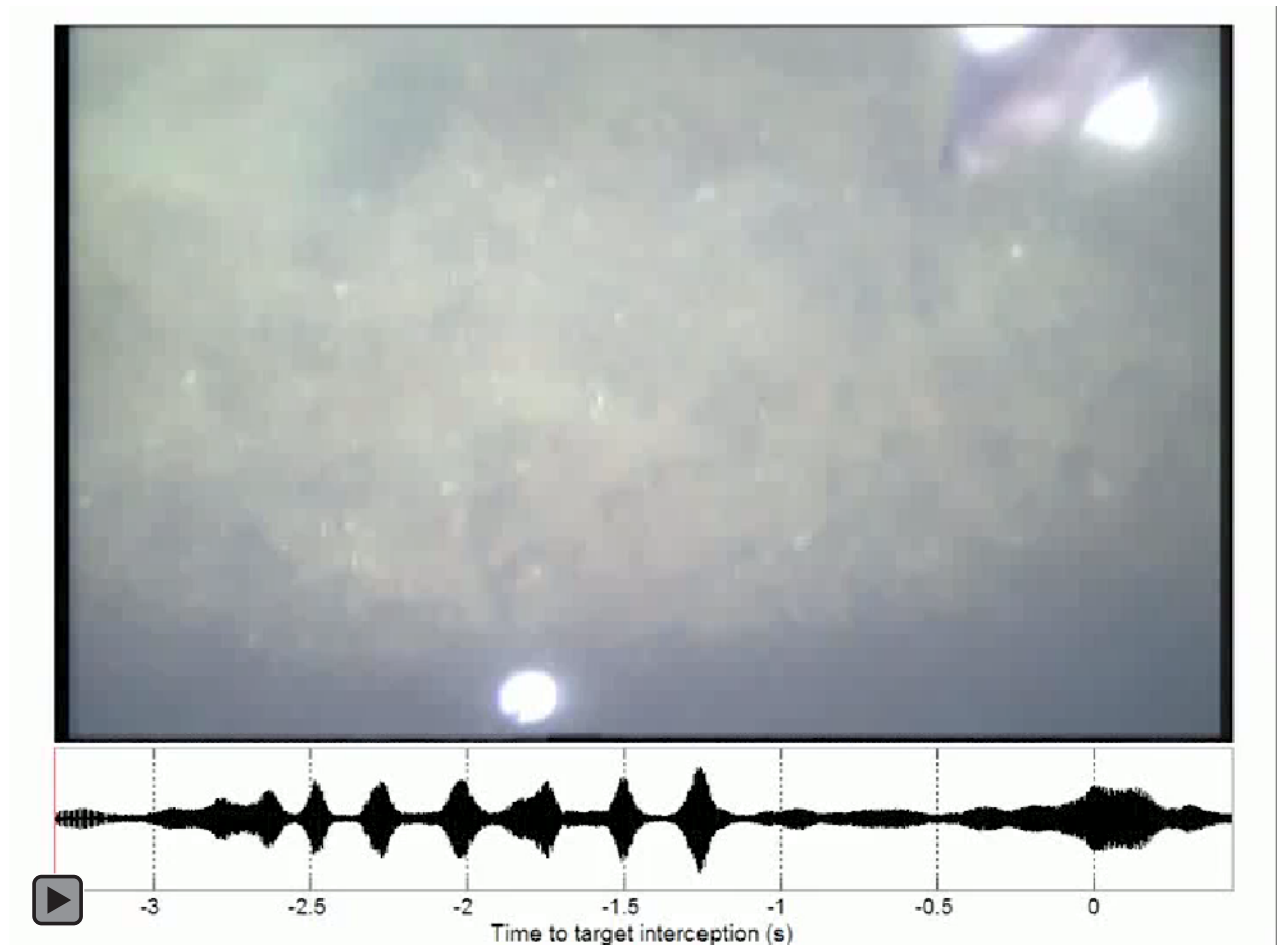


Fig. S6. Difference in received level (RL) between the standard and comparison targets plotted against target range for clicks recorded with both target hydrophones. Data from buzzes are limited because for the most part these were only recorded at the target towards which they were directed. (A) RL differences: $RL(\text{standard}) - RL(\text{comparison})$ versus $\text{range}(\text{standard})$ in red, and $RL(\text{comparison}) - RL(\text{standard})$ versus $\text{range}(\text{comparison})$ in black. The horn pattern results from the RL differences being smaller at long ranges and increasing at short ranges. This shows that initially, the animals were far enough that they could ensonify both targets simultaneously giving rise to high RLs on both targets. At shorter ranges, the animals could only ensonify one target at a time. (B) Normalized RL differences: $[RL(\text{standard}) - RL(\text{comparison})] / RL(\text{standard})$ in red and reversed in black, plotted to verify that the horn pattern does not result from the absolute levels at longer ranges being smaller.



Movie 1. A porpoise scanning across the target of choice during the terminal (buzz) phase of the approach. The lower panel shows a synchronized sound recording from a hydrophone located just above the target. The video, originally recorded at 25 frames s⁻¹, has been slowed down by a factor of five.